THE DISTRIBUTION OF FLARE HEIGHTS AS DERIVED FROM LIMB FLARES*

By R. G. Giovanelli† and Marie K. McCabe†

In recent papers, J. W. Warwick (1955) and Constance S. Warwick (1955) have discussed the heights of flares—the former by examining the distribution of apparent areas across the disk, and the latter by measuring heights of limb flares. Both analyses indicate that flares have heights of the order of $10–20 \times 10^3$ km; J. W. Warwick's height-frequency distribution is well represented by $\exp(-\beta h)$, where $\beta = 0 \cdot 492 \times 10^{-5}$ km, while C. S. Warwick's height distribution has a maximum at about 14×10^3 km.

While limb observations would appear to provide the more attractive method for deriving the flare height distribution, one of C. S. Warwick's difficulties has been the small number, 39, of limb flare observations available. Observations with the Sydney Lyot monochromator from April 6, 1956 to April 5, 1957 have enabled us to detect 90 flares whose tops projected beyond the limb, and this larger sample has been used for a flare height analysis in which uncertainties in the position of the base in front of or behind the limb have been avoided. Further, we have been able to show that the limb flares are the same type of event as observed on the disk, and this has enabled us to find the mean flare area corresponding to the derived mean height. Our observations include smaller flares than those analysed by Miss Warwick, so we may expect our mean height also to be less.

Observational Material

The Sydney Lyot monochromator is operated on a $\frac{1}{2}$ min cycle, a 16 mm diameter Hα image of the disk being recorded on Eastman Kodak IV–E film. While the small image size militates against high resolution, these observations allow all flares of area above about 20×10^{-6} of the Sun's hemisphere to be detected; most of the flares are, in fact, very small, of class 1–.

There are two main difficulties associated with the analysis of heights of flares at the limb:

(*a*) the identification of events at the limb as flares similar to those which are observed on the disk. In the present analysis we shall demonstrate the validity of the identification by comparing rates of limb and disk occurrences of flares;

(*b*) the measurement of the true height of a flare when the base of the flare is at an unknown or uncertain distance behind or in front of the limb. It is possible to avoid this difficulty by measuring only the distance by which a flare

* Manuscript received October 11, 1957.

† Division of Physics, C.S.I.R.O., University Grounds, Chippendale, N.S.W.

projects beyond the limb, irrespective of the position of its base, and using an appropriate analysis as described below.

During the above-mentioned 12 months' interval, covering a period around sunspot maximum, 90 events, classified as flares on the basis of their brightnesses and lifetimes, were observed with the top of the flare region projecting beyond the limb. For present purposes, the top of the flare has been taken as the limit of the region considered to be of flare brightness. We have specifically excluded fainter parts of brightness equal to those of the chromosphere or of the brighter projections such as stable plages, as well as the bright diffuse regions, ejected by some flares, which eventually fade to become dark surges. As a consequence, we believe that this analysis provides the height distribution for what are commonly accepted as normal flares.

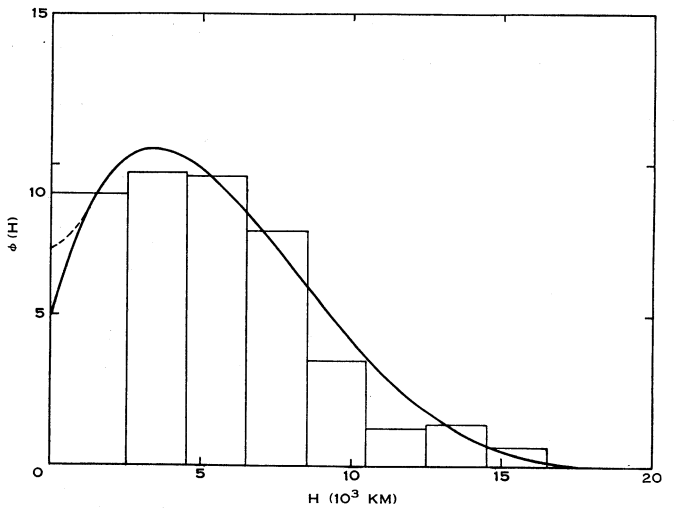

Fig. 1.—Histogram showing $\varphi(H)$, the observed number of flares, per 10^3 km projecting height H above the limb. The continuous curve shows the analytic function used to represent $\varphi(H)$, the dotted portion between $0 \leqslant H \leqslant 1 \cdot 19 \times 10^3$ km being the correction required to the analytic function to result in a zero value for the derived function $f(h)$ over the same range $0 \leqslant h \leqslant 1 \cdot 19 \times 10^3$ km.

The observed height distribution of the parts of these flares projecting beyond the chromosphere is shown in the histogram of Figure 1 ; the uncertainty of the individual measurements is believed to be of the order of 2×10^3 km.

Reduction of Observations

Let there be N flares per radian of longitude, of which $Nf(h)\mathrm{d}h$ have tops in a true height range h to $h+\mathrm{d}h$. If the radius vector from the flare to the centre of the Sun makes an angle θ with the perpendicular to the line of sight, the flare overlaps the limb by a projected distance

$$H=(R+h)\cos\theta-R, \quad \ldots\ldots\ldots\ldots\ldots \quad (1)$$

where R is the solar radius (Fig. 2).

Assuming that the Earth and the flares lie in the Sun's equatorial plane (a simplification that introduces little error), the number of flares in $\mathrm{d}\theta$, $\mathrm{d}h$ is given by $Nf(h)\mathrm{d}h\mathrm{d}\theta$, corresponding to which there will be $Nf(h)\mathrm{d}H\sec\theta\mathrm{d}\theta$ projecting beyond the limb in a projected height range $\mathrm{d}H$. The total number in $\mathrm{d}H$ is thus

$$\varphi(H)\mathrm{d}H=2N\mathrm{d}H\int_0^{\pi/2} f(h)\sec\theta\mathrm{d}\theta. \quad \ldots\ldots\ldots\ldots \quad (2)$$

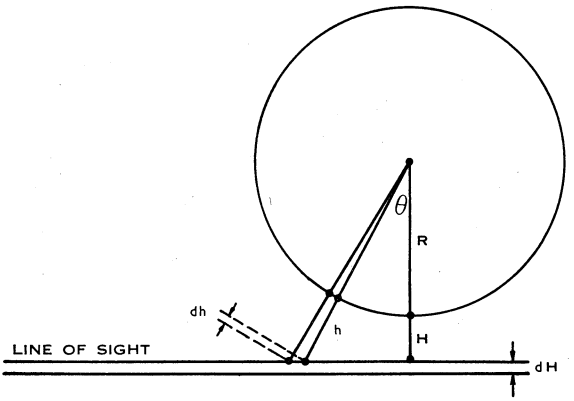

Fig. 2.—The geometrical relationship between the observed projected height H and the true height of a flare, h.

But the line of sight, (**1**), gives on differentiation

$$\mathrm{d}h=(R+h)\tan\theta\mathrm{d}\theta,$$

whence (**2**) becomes

$$\varphi(H)=2N\int_H^\infty \frac{f(h)\mathrm{d}h}{(R+h)\sin\theta}$$

$$=2N\int_H^\infty \frac{f(h)\mathrm{d}h}{\{(2R+h+H)(h-H)\}^{\frac{1}{2}}}.$$

Since $h+H\ll 2R$ for all significant cases,

$$\varphi(H)=\frac{2N}{(2R)^{\frac{1}{2}}}\int_H^\infty \frac{f(h)\mathrm{d}h}{(h-H)^{\frac{1}{2}}}. \quad \ldots\ldots\ldots\ldots\ldots \quad (3)$$

The solution of this integral equation for the flare height distribution $f(h)$ in terms of the radius R, the observed number of limb flares N, and the observed height distribution of the parts of flares projecting beyond the limb, $\varphi(H)$ (see Fig. 1), is obtained by assuming $f(h)$ expressible, over the range $0\leqslant h\leqslant K$ in which $f(h)$ has significant values, by a polynomial

$$f(h)=\Sigma a_n h^n,$$

and that $f(h)=0$, $h>K$. With a suitable change of variable, (**3**) then becomes

$$\varphi(H)=\alpha\int_0^{K-H}\Sigma a_n(x+H)^n\,.\,x^{-\frac{1}{2}}\mathrm{d}x, \quad \ldots\ldots\ldots \quad (4)$$

where $\alpha=N(2/R)^{\frac{1}{2}}$.

The integral in (4) can be evaluated term by term, yielding a series of half-integral powers of $(K-H)$. If we fit $\varphi(H)/(K-H)^{\frac{1}{2}}$ by a power series $\Sigma b_n H^n$, we can equate the coefficients of equal powers of H on either side of the expression resulting from (4), and these lead to a solution for the a_n in terms of the known b_n.

Now, the observed function $\varphi(H)$ is such that it drops effectively to zero at a height $H \approx 17 \cdot 5 \times 10^3$ km, so we choose $K = 17 \cdot 5 \times 10^3$ km. The function $\varphi(H)/(K-H)^{\frac{1}{2}}$ can be fitted by a polynomial of the fourth degree in H to within the limits of observational error, the corresponding curve $(K-H)^{\frac{1}{2}}\Sigma b_n H^n$ being superimposed on the histogram of Figure 1.

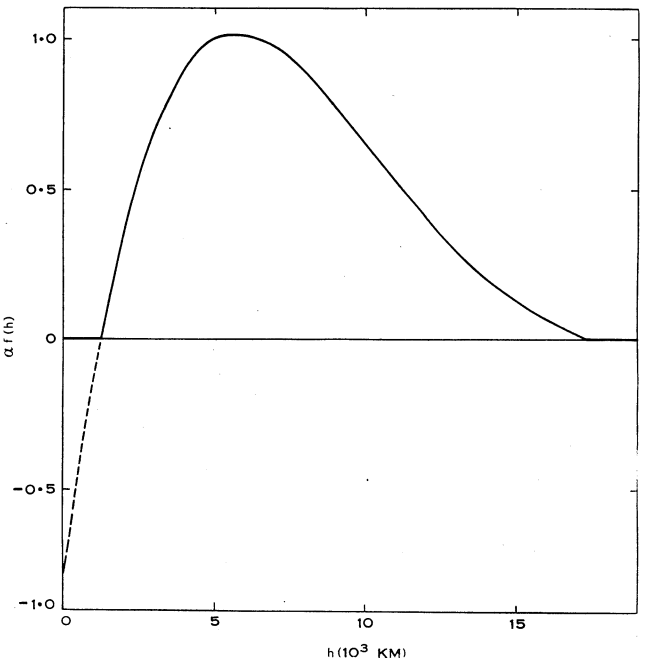

Fig. 3.—The derived flare height distribution $f(h)$ as a function of h. The ordinates are values of $\alpha f(h)$, where $\alpha = N(2/R)^{\frac{1}{2}}$.

The resulting solution, $f(h) = \Sigma a_n h^n$, is given in Figure 3. We may note that this function has negative values (dotted curve) near the origin, indicating the inadequacy of the power series $\Sigma b_n H^n$ near the origin. Actually, this is of little significance ; by allocating zero values to $f(h)$ for heights below $1 \cdot 19 \times 10^3$ km we affect only the correspondence with observed heights in the range 0–$1 \cdot 19 \times 10^3$ km, and in fact the required observed value of $\varphi(H)$ at $H = 0$ is $7 \cdot 2$, in better agreement with the histogram than the analytical curve at this point.

Discussion of Results

This analysis of limb flares leads to the real height distribution as shown in Figure 3, with flare heights lying between $1 \cdot 2 \times 10^3$ and $17 \cdot 5 \times 10^3$ km. The mean flare height is $7 \cdot 3 \times 10^3$ km ; the extremities of the distribution are unreliable because of the lack of resolving power and the limited observational data.

From these results, we can now calculate N, the number of flares per radian of longitude, with the result $N=331$. The total number of observable flares occurring in the period of observation should, on this basis, be πN + one-half the number of limb flares (those with bases behind the limb). The expected total is 1084, with a standard deviation, derived from a total of 90 limb flares, of $\sigma=\pm 115$; the analysis and the non-random nature of flare occurrences—in that they are associated with active centres—would increase σ somewhat. This total may be compared with an actual total of 1327 flares observed during the

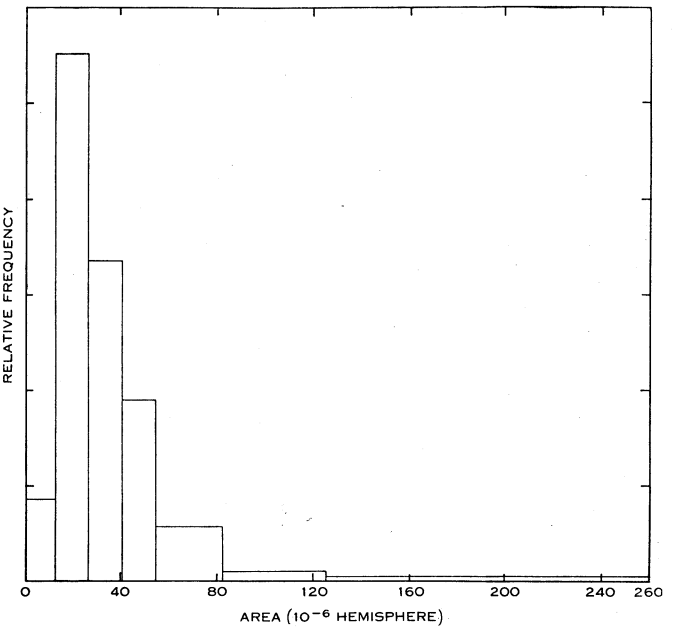

Fig. 4.—Histogram showing apparent area distribution for 269 flares occurring within 30° of the centre of the Sun's disk.

same period. The agreement is sufficiently good (within about 2σ) to justify our conclusion that the flares observed on the limb are the same type of event as those observed on the disk. In this case the area distribution applicable to flares near the centre of the disk should also be applicable to our limb flares. Figure 4 shows a histogram giving our observed distribution of apparent area for 269 flares occurring within 30° of the centre of the Sun's disk during part of the observation period; from this we deduce that the average area of these flares is about 40×10^{-6} of the Sun's hemisphere ($1\cdot2\times10^{8}$ km^2). As shown above, such a flare has an average height of $7\cdot3\times10^{3}$ km.

References

WARWICK, CONSTANCE S. (1955).—*Astrophys. J.* **121**: 385.
WARWICK, J. W. (1955).—*Astrophys. J.* **121**: 376.